

Portland State University

PDXScholar

Anthropology Faculty Publications and
Presentations

Anthropology

10-2013

Late Holocene Tsunami Deposits at Salt Creek, Washington, USA

Ian Hutchinson
Simon Fraser University

Curt D. Peterson
Portland State University, curt.d.peterson@gmail.com

Sarah L. Sterling
Portland State University

Follow this and additional works at: https://pdxscholar.library.pdx.edu/anth_fac



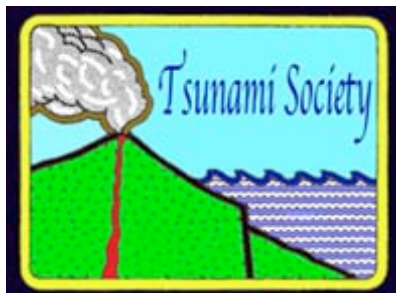
Part of the [Archaeological Anthropology Commons](#), [Geology Commons](#), and the [Tectonics and Structure Commons](#)

Let us know how access to this document benefits you.

Citation Details

Ian Hutchinson, Curt D. Peterson and Sarah L. Sterling (2013). Late Holocene tsunami deposits at Salt Creek, Washington, USA. *Science of Tsunami Hazards* vol. 32, pp. 221-235.

This Article is brought to you for free and open access. It has been accepted for inclusion in Anthropology Faculty Publications and Presentations by an authorized administrator of PDXScholar. Please contact us if we can make this document more accessible: pdxscholar@pdx.edu.



SCIENCE OF TSUNAMI HAZARDS

Journal of Tsunami Society International

Volume 32

Number 4

2013

LATE HOLOCENE TSUNAMI DEPOSITS AT SALT CREEK, WASHINGTON, USA

Ian Hutchinson

Geography, Simon Fraser University, Burnaby, BC, CANADA

Curt D. Peterson

Geology, Portland State University, Portland, OR, USA

Sarah L. Sterling

Anthropology, Portland State University, Portland, OR, USA

ABSTRACT

We interpret two thin sand layers in the estuarine marsh at Salt Creek, on the southern shore of the Strait of Juan de Fuca, as the products of tsunamis propagated by earthquakes at the Cascadia subduction zone. The sand layers extend for about 60 m along the left bank of the creek about 800 m from the mouth, and can be traced to the base of a nearby upland area. One layer is exposed in the creek bank about 400 m further upstream, but they are only patchily distributed in the rest of the central area of the marsh. Both layers contain brackish-marine epipsammic diatoms. The lower sand layer marks a sharp contact between intertidal peaty mud and overlying mud, perhaps reflecting modest coseismic subsidence in association with tsunami deposition, but little or no change in the bracketing sediment occurs in association with the upper sand layer. The ages of the sand layers are not closely constrained, but were most likely deposited by tsunamis generated by great earthquakes at the Cascadia subduction zone about 1650 and 1300 years ago. The Cascadia great earthquake of AD1700 may have induced slight subsidence in the marsh, but no tsunami deposit was detected at the inferred contact. The absence of deposits from the marsh immediately inland of the 4 m-high barrier beach indicates that the largest tsunamis in the late Holocene at this site have not overtopped the barrier, which suggests that these tsunamis were likely only 2-3 m high.

Key words: *tsunami deposits, diatoms, Cascadia subduction zone, Strait of Juan de Fuca, Washington*

Vol. 32, No. 4, page 221 (2013)

1. INTRODUCTION

The geological characterization of the deposits left by prehistoric tsunamis has become one of the principal tools for assessing tsunami risk in susceptible areas. Mapping and analysis of the deposits can be used to establish the spatial extent of inundation, the height of wave run-up, the current velocity, and the frequency of occurrence of these hazards at a coastal site. In areas where few historical tsunamis have occurred these deposits serve as warnings, alerting local residents, in Weiss and Bourgeois' (2012) words, to the fact that "it can and has happened here".

The Cascadia subduction zone (extending from Cape Mendocino in northern California to Vancouver Island; Fig. 1A) is one area where the absence of major tsunamis during the historical period (AD 1778 —) engendered a false sense of security amongst coastal residents. Recent investigations of the distribution and character of palaeo-tsunami deposits in coastal marshes and near-shore lakes have revealed, however, that the shorelines of Cascadia are at considerable risk from tsunamis generated by ruptures at the interface of the Juan de Fuca and America plates (Fig. 1A).

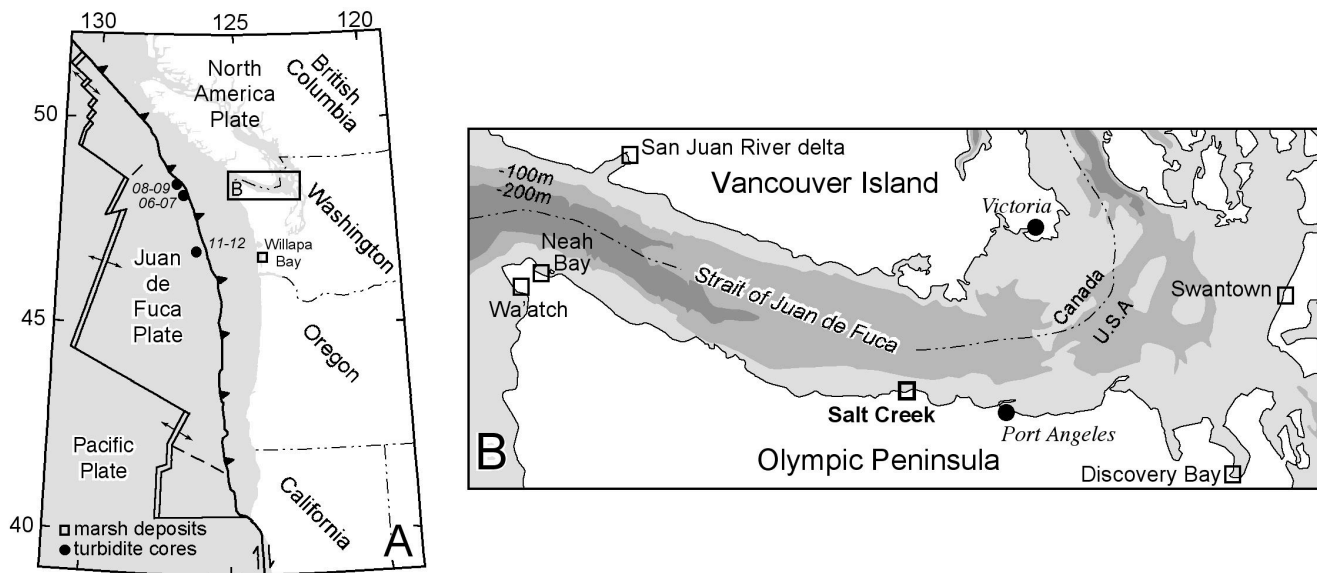


Fig. 1. (A) Major features of the Cascadia subduction zone, showing sites mentioned in the text, and (B) the Strait of Juan de Fuca, showing bathymetry and location of sites discussed in text. In A, the trace of the Cascadia thrust fault (dashed barbed line, barbs point down-dip) is placed at the bathymetric boundary between the continental slope and abyssal plain; double lines are spreading ridges, solid lines are strike-slip faults, and dashed lines are political boundaries.

Peters et al. (2003) listed 60 coastal sites in Cascadia that had been examined for evidence of tsunami inundation since the seismic potential of the Cascadia plate boundary was first recognized (Atwater, 1987; Heaton and Hartzell, 1987). The geographic distribution of these sites, however, is not uniform; whereas virtually all of the coastal marsh areas in southwestern Washington, Oregon and

California have been intensively investigated, and many of the marshes and lakes on the northwest and west-central coast of Vancouver Island have been examined, only a few sites (Williams and Hutchinson 2000, Williams et al. 2005, Peterson et al., 2013) have been investigated on the shores of the 160-km long Strait of Juan de Fuca, which connects the inland waters of Georgia Strait and Puget Sound to the Pacific Ocean (Fig. 1B).

In an attempt to remedy this situation, we describe the results of a search for paleotsunami deposits at an estuary on the southern shore of the strait, and place these results in the context of previous investigations of tsunami hazard in the region. We anticipate that these results will be of value in refining tsunami source models for the northern segment of the Cascadia subduction zone.

2. IDENTIFYING EPISODES OF COSEISMIC SUBMERGENCE AND PALEOTSUNAMI DEPOSITS

A variety of high-energy processes can leave anomalous elements in marsh deposits. Coarse-textured layers, such as sands or gravels, may be deposited by both fluvial and coastal processes. Material transported into a marsh by very large waves tends to have a characteristic sedimentary signature that distinguishes it from material left by river floods. Coarse layers left by tsunamis and storm surges tend to become finer and taper in thickness landward (Goto et al. 2012) and the number of layers diminishes landward as the inundation limit of individual events is passed. Moreover, these deposits commonly contain tell-tale microfossils reworked from offshore or neighboring beaches and tidal flats (Hemphill-Haley 1995, 1996). Distinguishing tsunami deposits from those left by storm surges is more difficult. Storms commonly leave thick washover deposits in the lee of overtopped beaches, and their deposits show more complex patterns of stratification than those of tsunamis (Morton et al. 2007, Peters and Jaffe 2010, Tuttle et al. 2004).

But the most compelling evidence of tsunami inundation is a layer of sand above a buried marsh soil that marks an episode of coseismic subsidence (e.g. Atwater 1997, Atwater et al. 2004). Plants growing in coastal marshes trap fine-grained sediment transported into the marsh by high tides. This material accumulates on the marsh surface, and the annual incorporation of decaying plant matter leads to the development of a peaty soil. If the subsidence accompanying a great earthquake locally exceeds about 0.5 m, the marsh surface may be lowered into the tidal flat zone, and the marsh soil is gradually buried by mud (e.g. Guilbault et al. 1996). A more modest amount of subsidence might lower the surface into the low marsh zone, characterized by the accumulation of slightly peaty mud. A regionally-coherent depositional sequence of buried marsh soils capped by mud layers (peat-mud couplets) is *prima facie* evidence of episodic coseismic deformation at subducting plate margins (Atwater 1997).

Not all the sandy layers at peat-mud contacts, however, are the products of tsunamis. Marsh deposits are commonly underlain by tidal flat sands, and these may be vented onto the marsh surface during major earthquakes. A liquefaction deposit may also contain marine microfossils, and can potentially be confused with tsunami-laid sands (Martin and Bourgeois 2012), particularly when sample cores are widely spaced.

3. STUDY SITE AND METHODS

The intertidal marsh at the mouth of Salt Creek on the south-central shore of the Strait of Juan de Fuca (48.16°N, 123.71°W; Fig 1B, 2A) currently occupies an area of about 22 ha. The marsh has developed in an intertidal embayment sheltered by a 4 m-high sandy barrier beach that is oriented WSW-ENE and is breached at its eastern end by the creek (Fig. 2B). Todd et al. (2006) note that the marsh was used as pasture in the decades following Euroamerican settlement, but disturbance was minor, and took the form of diking and ditching, particularly in the northwestern quadrant of the marsh.

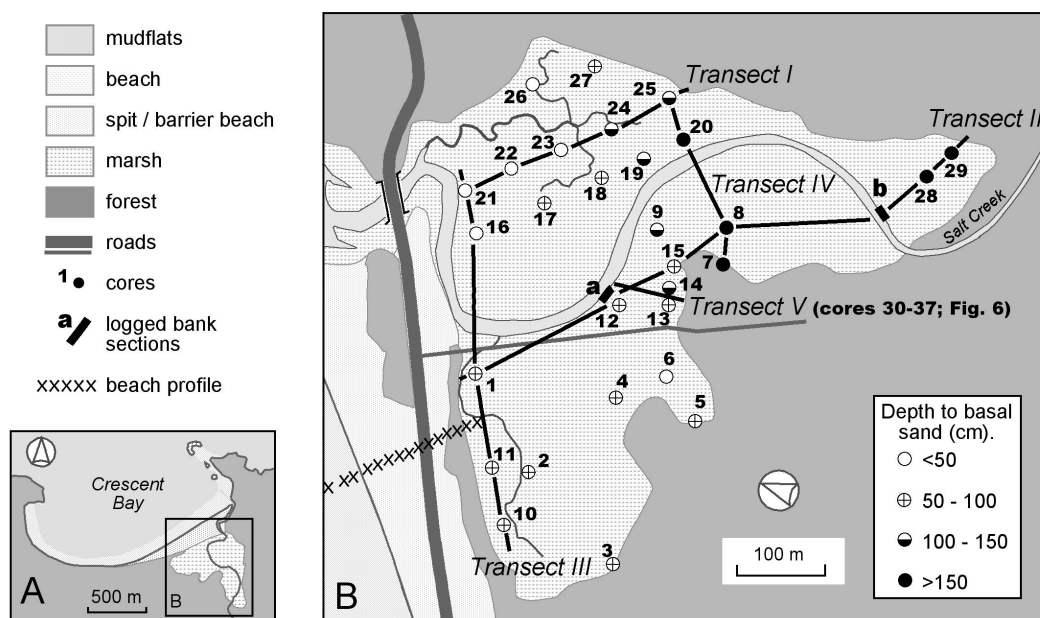


Fig. 2. (A) Salt Creek estuary and environs; (B) Salt Creek marsh, showing the location of core sites, the depth to basal sand in the cores and the location of the transects displayed in Figures 4 and 5.

We described the stratigraphy in the marsh deposits using a hand-driven gouge core (2m long, 2.5 cm wide) to retrieve samples, and examined exposures along the channel banks of Salt Creek for evidence of laterally continuous sand layers, focusing on two outcrops (Fig. 2B).

Three bench marks were established by RTK-GPS (± 5 cm) onsite. Core and bank outcrop locations were established by GPS using a Garmin 12-channel receiver with WASS real-time differential correction. A topographic profile was surveyed using a total station across the barrier beach and the eastern marsh to the upland margin. The barrier beach reaches a height of 4.0 m (NADV88 datum). The marsh surface lies just above MHHW in Crescent Bay, ranging in elevation from about 2.1 to 2.4 m at the core locations.

We collected samples of organic material (sticks, charcoal fragments, marsh peats) from cores and bank sections to date marsh initiation in the embayment and to constrain the age of paleotsunami

layers. Five samples were submitted to Beta Analytic for AMS dating. Conventional radiocarbon ages were calibrated with CALIB 6.0 using INTCAL09 data with the laboratory multiplier set to 1. The results (Table I) are rounded to the nearest decade.

Table I: AMS radiocarbon ages, Salt Creek marsh

core / outcrop	Depth (m)	Lab number (Beta-)	Material dated	14C age (yr BP)	Cal BP (2 sigma range)	significance
8	0.94	331750	plant material	940±30	930 — 790	rejected (root contamination)
a	0.60	355056	charcoal	1560±30	1530 — 1380	close maximum limiting age for upper sand at outcrop “a”
28	1.26	322473	peat	1590±30	1540 — 1410	maximum limiting age for marsh initiation near outcrop “b”
a	0.55	322471	peat	1790±30	1820 — 1620	maximum limiting age for upper sand at outcrop “a”
a	0.88	355055	stick	2330±30	2360 — 2330	maximum limiting age for marsh initiation and lower sand at outcrop “a”
a	0.69	322472	wood fragment	2440±30	2700 — 2360	maximum limiting age for lower sand at outcrop “a”

Samples for diatom analysis were collected from sand layers in the river bank and from a thick sand layer in one of the cores. A composite sample was taken from algal mats on sandy sediments in the vicinity of the mouth of the creek for comparative purposes. Organic matter in the samples was removed by H₂O₂ digestion. The remaining material was dispersed in 250 ml of distilled water, and, after repeated decanting and settling to remove fine sand to bring the solution to a near-neutral pH, aliquots of suspended material were dried on glass slides and mounted in Zrax. At least 300

specimens, or, in diatom-poor materials, the number of valves encountered on 10 random parallel traverses of the slide, were identified and counted for each sample (except the modern sample, which was qualitatively assessed). Identifications of taxa were principally based on descriptions in Hemphill-Haley (1993) and Witkowski (2000).

3.1 Paleoseismic and tsunami evidence at Salt Creek

River bank sections - Two thin but continuous layers of sand are readily evident on the left bank of Salt Creek, about 800 m from the mouth, as a result of etching by high tides. The sand layers extend from about 10 m downstream of site “a” to about 50 m upstream of the site (Fig. 3). They lie in the middle of the bank section, about 0.1 m apart (Fig. 4A). The sand layers are more-or-less horizontal, of uniform thickness, and display sharp contacts with the encasing fine-grained deposits (Fig. 4B).



Fig. 3. Left bank of Salt Creek upstream of riverbank section “a” (at right of photo). The two sand layers in the bank are visible as parallel etched lines [photo: Brian Atwater].

Along this section of the bank a basal channel or tidal flat sand at a depth of 1.2 m is sharply overlain by mud, with peaty mud and muddy peat phases becoming more prominent towards the top (Fig. 4A). The lower sand layer (at 0.7 m depth in the logged section) is underlain by a 3-cm thick layer of grayish-brown peaty mud, and overlain by a less peaty gray mud. The former likely represents an incipient high intertidal marsh, the latter a low marsh environment. The abrupt change from incipient high marsh to low marsh may signal a modest amount (<0.5 m) of submergence, either as a result of coseismic settling and compaction, or elastic tectonic subsidence.

There is a less pronounced change in the deposits bracketing the upper sand (at 0.6 m depth in the logged section), suggesting a smaller degree of coseismic subsidence. The only other potential subsidence event displayed in this section occurs at a depth of about 0.3 m, where a dark brown muddy peat is abruptly overlain by tan to yellowish brown mud, perhaps indicating a subsidence event equivalent to that recorded at in association with the lower sand layer.

Both sand layers were about 5 mm thick throughout this section of the river bank. Both were composed of fine to very fine sand. Their lateral extent and uniform thickness, and the absence of

sand dikes in the underlying muds indicate that they are not the products of liquefaction. They may be the products of extreme storms, but the distance of the outcrop from the mouth of the creek argues against that interpretation. The association between the lower sand and (albeit weak) evidence of coseismic subsidence suggests that it is likely a tsunami deposit, and the very similar character of the upper sand bed suggests that it is also the product of a tsunami.

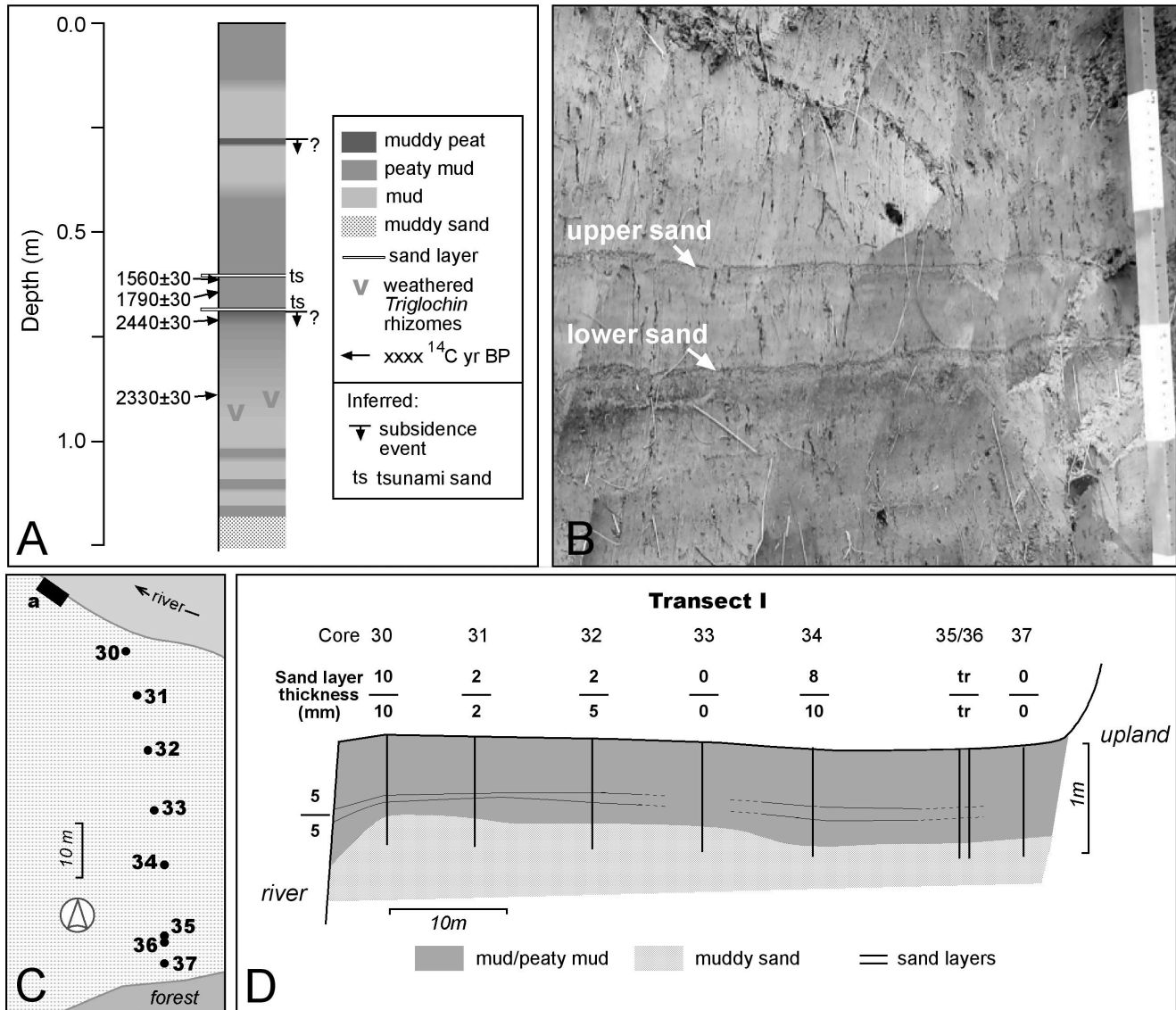


Fig. 4. (A) Lithology, radiocarbon ages, and inferred seismic events at riverbank section “a” at Salt Creek; (B) Closeup of the two sand layers at the logged section, showing the incipient high marsh peat layer beneath the lower sand. Divisions on the measuring stick are 10 cm long [photo: Brian Atwater]; (C) Location of cores along transect I; (D) Simplified lithology of cores on Transect I, showing the depth and thickness of the two inferred tsunami sand sheets.

Both sand beds had similar assemblages of diatoms, with epipellic marsh taxa dominant. The absence of freshwater species in the diatom assemblage shows that the sand beds are not fluvial deposits. The commonest species (~50-70% of the total count) is *Diploneis interrupta*. A large percentage of the frustules of this species were intact and unweathered. *Diploneis interrupta* is a salt marsh diatom with a large salinity tolerance range (Vos and de Wolf 1993), and although Hendey (1964) notes that it is also commonly found on sandy beaches, it was absent from the sample taken at the mouth of Salt Creek. That observation, the pristine condition of the frustules of *D. interrupta*, and the presence of *Cosmioneis pusilla* and *Caloneis westii*, which are also absent from the river-mouth sample, suggest that this assemblage is largely a product of post-depositional colonization of the surface of the sand by epipellic marsh diatoms.

In addition to the epipellic marsh taxa there are, however, small numbers (~5% of the total count) of brackish-marine epipsammic taxa (principally *Trachysphenia australis*, *Delphineis minutissima* and *Opephora mutabilis*) in both sand beds. These diatoms typically grow on sandy substrates in the lower intertidal or shallow subtidal zone (Vos and de Wolf 1993, Witter et al. 2009), and they may have been transported with the sand from near-shore habitats to the high marsh. Their presence supports our contention that the sand layers are the product of tsunami deposition. Their low relative abundance (compared, for example, to the results reported by Hemphill-Haley, 1996), is likely a product of not being able to sample the centre of these very thin sand beds, thereby including the post-depositional colonists.

The ages of the sand beds are constrained by four radiocarbon samples collected from the logged section and its immediate vicinity (Table I). These supply maximum limiting ages for the inferred tsunamis. A stick lying immediately above weathered rhizomes of *Triglochin maritima* at about 0.9 m depth (0.2 m below the lower sand layer) yielded an age of 2400 –2300 cal. yr BP. Both sand layers therefore post-date this period. A charcoal fragment from the mud at the base of the upper sand indicates that this layer was deposited about, or shortly after, 1530–1380 cal. yr BP. The lower sand layer almost certainly dates from the intervening interval.

At riverbank site “b” (Fig. 2B), 400 m further upstream, a thin layer (5 – 15 mm thick) of fine to very fine sand occurs at 0.7 m depth (Fig. 5; Transect III), the same depth as the lower sand at site “a”. The correlation with the lower sand is tentative, however, because the continuity of the sand layers is interrupted by outcrops of point bar deposits in the channel banks between the two sites. A diatom sample from this sand was barren.

Stratigraphy: cores - We attempted to determine the inland extent of tsunami inundation in the vicinity of logged section “a” by tracing the two sand beds from the riverbank to the base of a small upland promontory about 60 m away (Fig. 2B; Transect I). The extent and thickness of the two sand layers in the rest of the marsh was determined from a further 29 cores (Fig. 2B).

A series of simplified sedimentary sections (Figs. 4C, 5) show the results of the coring program. In all the cores a basal tidal flat or channel sand fines up-core to mud, peaty mud, muddy peat, and, in a few instances, peat (>50% organic matter), marking the gradual infilling of the Salt Creek embayment in the late Holocene.

In Transect I the two sand layers can be traced from the riverbank for about 50 m inland in the 1 m-thick peaty mud facies that caps the intertidal sands. The sand beds are thickest (10 mm) in the core closest to the riverbank (Fig. 4C), and taper inland, but thicken again at one site in the lee of the raised

channel margin. They thin to single-grain thickness at the base of the upland, which likely marks the inundation limit.

In the northeast quadrant of the marsh (Fig. 5, Transect II) the cap of mud and peaty mud is <0.5 m thick, and no evidence of abrupt changes in facies or anomalous sand layers were detected in this area. About 200 m inland, however, the surficial mud and peaty mud units rapidly thicken, reaching 1.5 m close to the upland margin of the marsh. Cores close to this upland margin display abrupt but subtle changes in lithology, and very thin sand layers were noted at depths akin to those in logged section “a”.

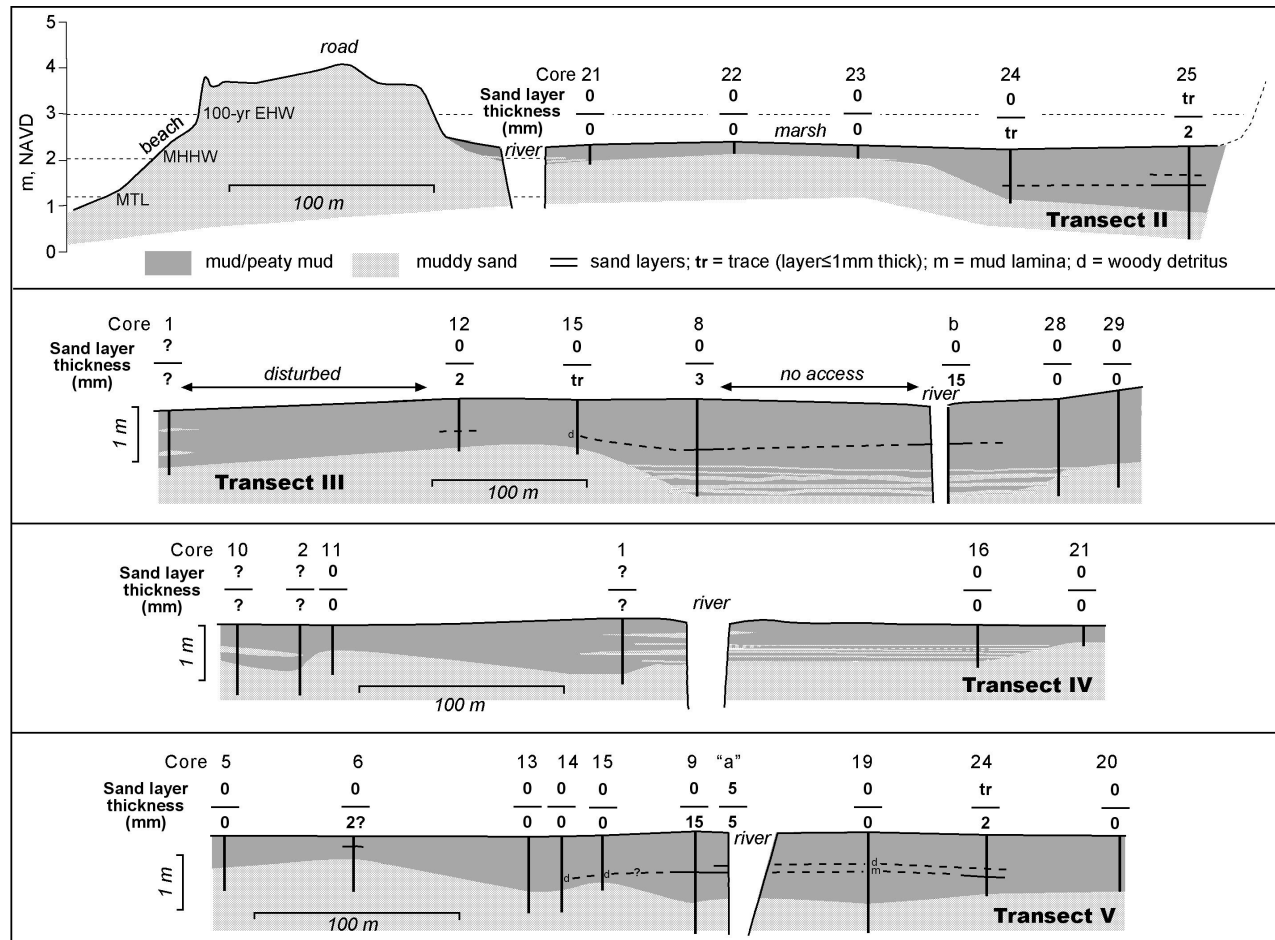


Fig. 5. Stratigraphy of cores along two shore-orthogonal transects (II and III), and two shore-parallel transects (IV and V), at Salt Creek marsh. The location of the transects is shown in Fig. 2B.

Transect III (Fig. 5) illustrates the variation in deposits in the western part of the marsh, and in a marsh embayment upstream. No sand beds were detected in the mud and muddy peaty units of the two cores landward of riverbank section “b” (Fig. 5; Transect III, cores 28, 29), but a thin sand bed occurs in the peaty mud facies in two of the cores close to section “a” (i.e. cores 12, 8). We noted a

layer of detrital wood fragments at an equivalent depth (0.7 m) in core 15. We tentatively correlate this sand-detritus bed with the lower sand in the nearby riverbank. A thicker layer of muddy sand occurs at 0.9 m depth in core 8. The few diatoms found in a sample from this layer were marsh and tidal flat taxa (Appendix II), and we consider this layer to be the uppermost of a series of channel/tidal flat sand deposits that interdigitate with mud at depths > 1m in core 8, riverbank section “b”, and core 28.

The basal sand in the cores along the shore-parallel transect immediately landward of the barrier beach (Fig. 5; Transect IV) typically lies at a depth of 0.6 —1.0 m. This fines into a thick mud or slightly peaty mud, which is capped by a thin dark brown peaty mud or peat. Two of the cores along this transect display anomalous sand layers (cores 1, 2) at similar depths. In core 1, a 3-cm thick sand layer lies at a depth of about 0.2 m below the surface, and a 9-cm thick layer of muddy sand lies at a depth of about 0.65 m, underlain by mud. The upper layer may be a product of disturbance associated with ditching of the marsh in this area, but the lower sand layer may be correlative with one of the two inferred tsunami layers in the logged riverbank section.

In core 2 this lower muddy sand layer is 6-cm thick and grades upwards into mud. The diatom assemblage in the muddy sand unit is dominated by species that live on muddy sandy shoals in the intertidal zone (*Planothidium delicatulum*, *P. hauckiana*, *Fallacia oculiformis*, *Opephora* spp., *Paralia sulcata*), so we consider it unlikely to be a tsunami deposit. The abrupt change between the sand layer and the underlying mud may therefore be a product of changes in the position of the meandering channel of Salt Creek, but it may also correlate with the subsidence event associated with the lower sand layer in the logged riverbank section.

Two of the cores discussed previously (cores 8, 25) are end-members of Transect V (Figure 5). The two intervening cores (7, 20) both show possible evidence of at least one weak subsidence event, and, in the case of core 7, a very thin (0.2-cm thick) sand layer at a depth of about 1.0 m that may correlate with the lower sand in the riverbank.

3. CONCLUSIONS AND IMPLICATIONS

In the near-shore areas of the Salt Creek marsh, extending landward for a distance of about 200 m from the inland margin of the barrier beach, the cap of muds and peaty muds above the tidal-flat deposits is thin, and has accumulated recently, most probably in the historic period. With one possible exception (Fig. 5; Transect V, core 1) the sedimentary archives in this area do not display evidence of the effects of prehistoric great earthquakes at the Cascadia subduction zone. The area that lies >600 m from the barrier beach also appears to be devoid of coseismic evidence, likely because the amount of subsidence at Salt Creek is too small to produce discernable changes in the character of the sediment in marsh areas close to the extreme limit of tides.

Facies changes are evident, however, in the intervening marsh area, primarily in the vicinity of the river channel. At least two such buried marsh soils can be detected in the logged riverbank section at Salt Creek. The lower horizon dates from the 2300 – 1530 cal yr. BP interval. The upper buried soil (at 0.3 m depth) is undated, but sharp facies changes at the same depth in the Wa’atch wetlands (Peterson et al., 2013) and on the San Juan River delta (Clague et al. 2000) date from the last plate-boundary earthquake in AD 1700, and we conjecture that the upper buried soil in the riverbank at Salt Creek also dates from this event.

The two sand layers identified in riverbank section “a” at Salt Creek as tsunami deposits are generally thicker than their counterparts in the cores from the rest of the marsh. This indicates that both tsunamis likely surged upriver, overtopped the channel banks, and spread across the marsh surface, leaving thin and patchy layers of sand and organic detritus in their wake.

We have no evidence to suggest that the 4 m-high barrier beach was overtopped by these waves. This implies that the maximum wave height did not exceed 3 m if the state of tide was close to MTL (~1 m NAVD88) when the biggest waves arrived, but must have exceeded 2 m in order to inundate the marsh surface. Tsunami simulation models developed by Cherniawsky et al. (2007) and AECOM Canada Ltd. (2013) generate maximum wave heights in the vicinity of Crescent Bay of about 2.5 m, which accords with our estimate.

If the two sand layers at Salt Creek are indeed the products of tsunamis prompted by ruptures at the Juan de Fuca – North America plate boundary, which events were responsible? Correlating the age of the inferred tsunami deposits at Salt Creek with the great-earthquake chronologies developed from buried marsh soil sequences in Willapa Bay (Fig. 1; Atwater and Hemphill-Haley, 1997), and turbidite sequences in Juan de Fuca and Barkley canyons (Fig. 1; Goldfinger et al., 2012), is complicated by the relatively poor dating control at Salt Creek, but it seems most likely (see Fig. 6) that the sand layers are products of plate-boundary earthquakes about 1650 years ago (event S in the Willapa Bay sequence), and about 1300 years ago (event U in the Willapa Bay sequence). These events are also the only well-documented tsunami deposits at Swantown marsh at the eastern end of the Strait of Juan de Fuca (Fig. 1B).

It is not surprising that deposits associated with the tsunami generated by the plate-boundary earthquake about 1650 years ago are widespread in marshes on the shores of the Strait of Juan de Fuca (Fig. 6). This earthquake followed a protracted period (about 1000 years) of strain build-up at the northern end of the Cascadia subduction zone, and the resultant thrust event was almost certainly larger than any other in the late Holocene.

The subsequent earthquake, however, followed only about 350 years of strain at the plate interface. Why are tsunami deposits attributable to this event found at Salt Creek, but those of subsequent plate ruptures not, despite the fact that they are encountered at Wa’atch – Neah Bay and Discovery Bay?

We suggest two possible reasons for this, operating singly or in concert:

1. The 1300 cal yr. BP tsunami coincided with high tide at Salt Creek; more recent tsunamis did not;
2. Changes in the morphology of the barrier beach in Crescent Bay led to narrowing of the river mouth within the last millennium, inhibiting tsunami incursion.

Tidal state – The last great earthquake at the Cascadia subduction zone is reliably dated to the January 26, AD 1700, at about 2100 h local time. Mofjeld et al. (1997) reconstructed the tidal state at that time, and concluded that the earthquake occurred during a low neap tide, which may explain the absence of a tsunami deposit from this event both at Salt Creek and Swantown marsh. The presence of tsunami deposits from the AD 1700 earthquake and preceding events at an intervening site (Discovery Bay) is almost certainly the result of wave amplification in that embayment (Cherniawsky et al., 2007).

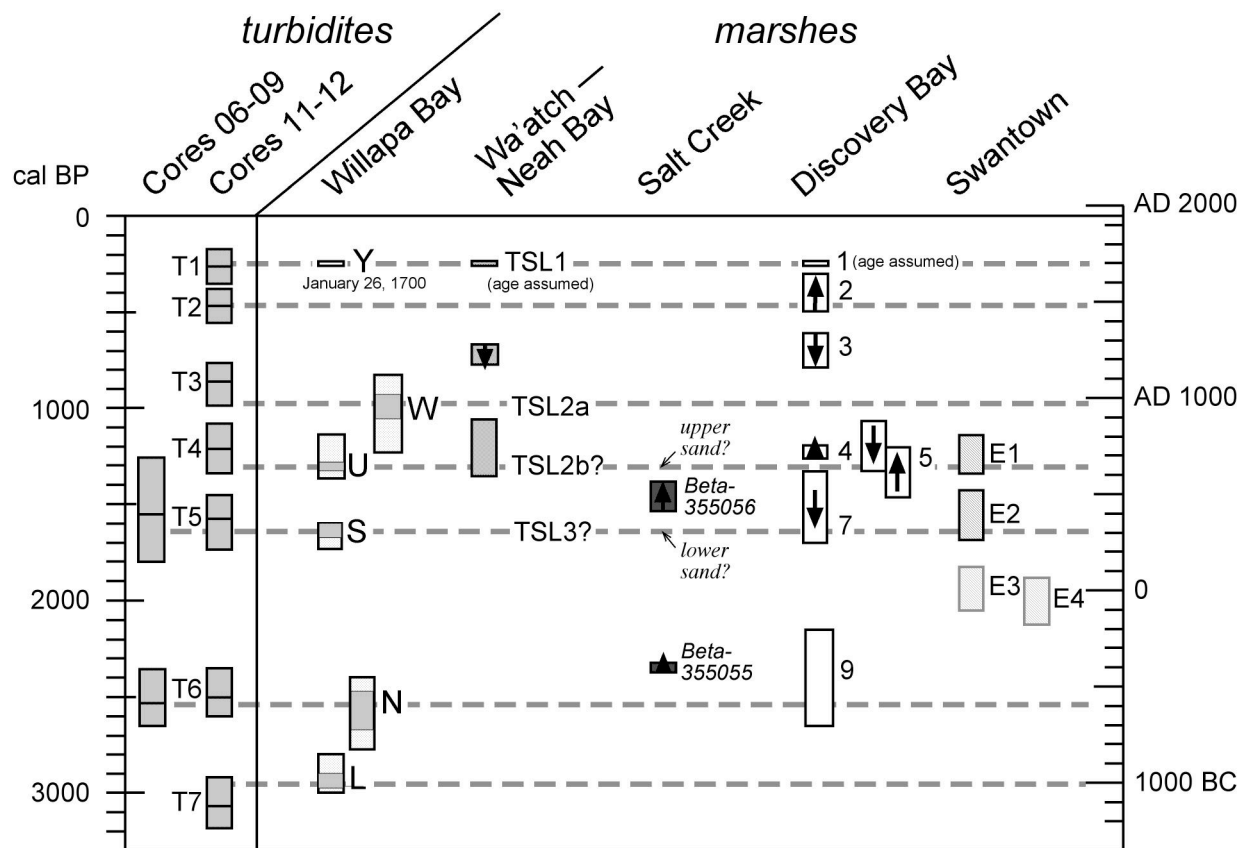


Fig. 6. Correlations between inferred paleotsunami events at Salt Creek marsh with paleoseismic and paleotsunami evidence from elsewhere in the Strait of Juan de Fuca and vicinity. Upward-pointing arrows indicate maximal ages; downward-pointing arrows indicate minimal ages. Data: turbidite cores (Goldfinger et al., 2012); Willapa Bay buried marsh soils (Atwater et al., 2004); Wa'atch – Neah Bay (Peterson et al., 2013); Discovery Bay (Williams et al., 2005), and Swantown marsh (Williams and Hutchinson, 2000).

Estuarine palaeogeography – Tsunami incursion up-channel at Salt Creek in the late Holocene has undoubtedly been influenced by the position and morphology of the barrier beach and the position and width of the mouth of Salt Creek. These in turn are influenced by regional climate (e.g. changes in storminess or river flooding regime), and relative sea level.

Relative sea level along the Cascadia littoral rises and falls as stress is built-up and released at the interface of the Juan de Fuca and North America plates. Incomplete release of stress in the earthquake phase of the cycle may have led to gradual tectonic uplift and lowering of local sea level, or, if the rate of uplift was more modest, offset of the eustatic sea level rise in the late Holocene and sea-level stabilization. Both of these scenarios would lead, in turn, to infilling of the back-barrier lagoon, reduction of the tidal prism, narrowing of the river mouth, and reduced tsunami access.

ACKNOWLEDGEMENTS

This project was funded by a Portland State University Faculty Enhancement Grant to Sarah Sterling. Thanks to our field assistants, Andrew Huff and Christopher Milton, and to the PSU Geology students (Charles Davidshofer, Scott Lunski, Molly Pontifex, Ann Stransberry, Emily Jenkins, Tamara Linde, Elizabeth Westby, Al Mowbray, and Craig Annsa) who undertook the elevation survey. Nan Feagin, Bud Taggart, the Luthers, the Palzers, and the Novaks allowed access to their land, and Anne Schaffer and Dave Parks gave us access, data, and encouragement. We particularly appreciate Brian Atwater's insights and guidance in the field, Josef Cherniawsky's sharing of tsunami model output, and Ian Miller's outreach efforts.

REFERENCES

- AECOM Canada Ltd. 2013. Modelling of Potential Tsunami Inundation Limits and Run-up. Report prepared for the Capital Regional District. Available online at <http://www.crd.bc.ca/media/documents/20130424-TsunamiFullreport.pdf> (accessed 13 August 2013).
- Atwater B. F. 1987. Evidence for great Holocene earthquakes along the outer coast of Washington State. *Science* 236:942-944.
- Atwater, B. F. 1997. Coastal evidence for great earthquakes in western Washington. U.S. Geological Survey, Professional Paper 1560:77-90.
- Atwater, B. F., and E. Hemphill-Haley. 1997. Recurrence intervals for great earthquakes of the past 3,500 years at northwestern Willapa Bay, Washington. U.S. Geological Survey, Professional Paper 1576.
- Atwater, B. F., M. P. Tuttle, E. S. Schweig, C. M. Rubin, D. K. Yamaguchi, and E. Hemphill-Haley. 2004. Earthquake recurrence inferred from paleoseismology. *Developments in Quaternary Science* 1:331-350.
- Clague, J.J., P. T. Bobrowsky, and I. Hutchinson, I., 2000. A review of geological records of large tsunamis at Vancouver Island, British Columbia, and implications for hazard. *Quaternary Science Reviews* 19:849–863.
- Cherniawsky J. Y., V. V. Titov, K. Wang, and J.-Y. Li. 2007. Numerical simulations of tsunami waves and currents for southern Vancouver Island from a Cascadia megathrust earthquake. *Pure and Applied Geophysics* 164:465–492.
- Goldfinger, C., C. H. Nelson, A. E. Morey, J. E. Johnson, J. R. Patton, E. Karabanov, J. Gutiérrez-Pastor, A. T. Eriksson, E. Gràcia, G. Dunhill, R. J. Enkin, A. Dallimore, and T. Vallier. 2012. Turbidite event history – methods and implications for Holocene palaeoseismicity of the Cascadia subduction zone. U.S. Geological Survey, Open-File Report 1661-F.

Goto, K., C. Chague-Goff, J. Goff, and B. Jaffe. 2012. The future of tsunami research following the 2011 Tohoku-oki event. *Sedimentary Geology* 282:1-13.

Guilbault, J. P., J. J. Clague, and M. Lapointe. 1996. Foraminiferal evidence for the amount of coseismic subsidence during a late Holocene earthquake on Vancouver Island, west coast of Canada. *Quaternary Science Review* 15:913-937.

Heaton, T. H., and S.H. Hartzell. 1987. Seismic hazards on the Cascadia subduction zone. *Science* 236:162-168.

Hendey, N. I. 1964. An Introductory Account of the Smaller Algae of British Coastal Waters. Part V: Bacillariophyceae (Diatoms). Ministry of Agriculture, Fisheries and Food, Fisheries Investigations Series IV. London.

Hemphill-Haley, E. 1993. Taxonomy of recent and fossil (Holocene) diatoms (Bacillariophyta) from northern Willapa Bay, Washington. U.S. Geological Survey, Open-File Report 93-289.

Hemphill-Haley, E. 1995. Diatom evidence for earthquake-induced subsidence and tsunami 300 yr ago in southern coastal Washington. *Bulletin of the Geological Society of America* 107:367-378.

Hemphill-Haley, E. 1996. Diatoms as an aid in identifying tsunami deposits. *The Holocene* 6:439-448

Martin, M. E., and J. Bourgeois. 2012. Vented sediments and tsunami deposits in the Puget lowland, Washington – differentiating sedimentary processes. *Sedimentology* 59:419-444

Mofjeld, H. O., M. G. G. Foreman, and A. Ruffman. 1997. West Coast tides during Cascadia subduction zone tsunamis. *Geophysical Research Letters* 24:2215-2218.

Morton, R. A., G. Gelfenbaum, and B. E. Jaffe. 2007. Physical criteria for distinguishing sandy tsunami and storm deposits using modern examples. *Sedimentary Geology* 200:184-207.

Peters, R., B. Jaffe, G. Gelfenbaum, and C. Peterson. 2003. Cascadia tsunami deposit database. U.S. Geological Survey, Open-File Report 03-13.

Peters, R., and B. Jaffe. 2010. Identification of tsunami deposits in the geologic record: developing criteria using recent tsunami deposits. U.S. Geological Survey, Open-File Report 2010-1239.

Peterson, C. D., K. M. Cruikshank, M. E. Darienzo, G. C. Wessen, V. L. Butler, and S. L. Sterling. 2013. Coseismic subsidence and paleotsunami run-up records from latest Holocene deposits in the Waatch Valley, Neah Bay, northwest Washington, U.S.A.: links to great earthquakes in the northern Cascadia margin. *Journal of Coastal Research* 29:157-172.

- Todd, S., N. Fitzpatrick, A. Carter-Mortimer, and C. Weller C. 2006. Historical changes to estuaries, spits, and associated tidal wetland habitats in the Hood Canal and Strait of Juan de Fuca regions of Washington State: Final Report. Appendix B2--central Strait region. PNPTC Technical Report 06-1, Point No Point Treaty Council, Kingston, Washington. Available online at http://www.pnptc.org/PNPTC_Web_data/Publications/habitat/GIS/Historic%20Changes%20Main%20Report.pdf (accessed 26 August 2012)
- Tuttle, M. P., A. Ruffman, T. Anderson, and H. Jeter. 2004. Distinguishing tsunami from storm deposits in eastern North America: the 1929 Grand Banks tsunami versus the 1991 Halloween storm. *Seismological Research Letters* 75:117-131.
- Vos, P., and H. de Wolf. 1993. Diatoms as a tool for reconstructing sediment environments in coastal wetlands – methodological aspects. *Hydrobiologia*, 269/270:285-296.
- Weiss, R., and J. Bourgeois. 2012. Understanding sediments – reducing tsunami risk. *Science* 336:1117.
- Williams, H., and I. Hutchinson. 2000. Stratigraphic and microfossil evidence for late Holocene tsunamis at Swantown marsh, Whidbey Island, Washington. *Quaternary Research* 54:218-227.
- Williams, H. F. L., I. Hutchinson, and A. Nelson. 2005. Multiple sources for late-Holocene tsunamis at Discovery Bay, Washington State, USA. *The Holocene* 15:60–73
- Witkowski, A., H. Lange-Bertalot, and D. Metzeltin. 2000. Diatom Flora of Marine Coasts I. *Iconographica Diatomologica* (volume 7), Koeltz Scientific, Koenigstein.
- Witter, R. C., E. Hemphill-Haley, R. Hart, and L. Gay. 2009. Tracking prehistoric Cascadia tsunami deposits at Nestucca Bay, Oregon. Final Technical Report, U.S. Geological Survey, National Earthquake Hazards Reduction Program, Award No. 08HQGR0076.